ORIGINAL ARTICLE

Obesity Biology and Integrated Physiology

Obesity | THE OBESITY SOCIETY | **WILEY**

p38α in the preoptic area inhibits brown adipose tissue thermogenesis

Jing Wang[1,2,3,4] | Shanshan Wu[1,2,3,4] | Huidong Zhan[1,2,3,4] | Wenkai Bi[1,2,3,4] | Yang Xu[1,2,3,4] | Yixiao Liang[1,2,3,4] | Yueping Ge[1,2,3,4] | Li Peng[1,2,3,4] | Xinchen Jin[1,2,3,4] | Keke Lu[1] | Jiajun Zhao[1,2,3,4,5] | Ling Gao[1,2,3,4,5] | Zhao He[1,2,3,4,6]

[1]Department of Endocrinology, Medical Integration and Practice Center & Shandong Provincial Hospital, Cheeloo College of Medicine, Shandong University, Jinan, China

[2]Shandong Key Laboratory of Endocrinology and Lipid Metabolism, Jinan, China

[3]Shandong Clinical Research Center of Diabetes and Metabolic Diseases, Jinan, China

[4]Shandong Prevention and Control Engineering Laboratory of Endocrine and Metabolic Diseases, Jinan, China

[5]Department of Endocrinology, Shandong Provincial Hospital Affiliated to Shandong First Medical University, Jinan, China

[6]Key Laboratory of Cardiovascular Remodeling and Function Research, Chinese Ministry of Education and Chinese Ministry of Public Health, Qilu Hospital, Cheeloo College of Medicine, Shandong University, Jinan, China

Correspondence

Ling Gao, Department of Endocrinology, Shandong Provincial Hospital, 324 Jingwu Road, Jinan, Shandong 250021, China.
Email: linggao@sdu.edu.cn

Zhao He, Shandong Provincial Hospital, Cheeloo College of Medicine, Shandong University, 544 Jingsi Road, Jinan, Shandong 250021, China.
Email: zhaohe@sdu.edu.cn

Abstract

Objective: Elevation of energy expenditure through an increase of brown adipose tissue (BAT) thermogenesis is regarded as one of the most promising ways to prevent obesity development. The preoptic area (POA) of the hypothalamus is a critical area for control of BAT thermogenesis. However, the intracellular signaling cascades in the POA for regulation of BAT thermogenesis are poorly understood.

Methods: Phosphorylation proteomics (phosphoproteomics) and bioinformatics approaches were used to disclose numerous hypothalamic signaling pathways involved in the regulation of BAT thermogenesis. Conditional manipulation of the p38α gene in mouse POA was performed by stereotaxic injection of adeno-associated virus 9 vector to explore the role of p38α in BAT thermogenesis.

Results: Multiple hypothalamic signaling pathways were triggered by cold exposure, especially the mitogen-activated protein kinase (MAPK) signaling pathway. The p38α activation, but not extracellular signal-regulated kinase 1/2 (ERK1/2) and c-Jun NH2-terminal kinase (JNK), in the hypothalamus was significantly decreased during cold exposure. p38α deficiency in the POA dramatically elevated energy expenditure owing to a marked increase in BAT thermogenesis, resulting in significantly decreased body weight gain and fat mass. Overexpression of p38α in the POA led to a dramatic increase in weight gain.

Conclusions: These results demonstrate that p38α in the POA exacerbates obesity development, at least in part owing to a decrease in BAT thermogenesis.

INTRODUCTION

Obesity has become an epidemic disorder in recent decades [1]. Energy intake, more than energy expenditure, is the fundamental cause of obesity development [2]. Therefore, elevation in energy expenditure is considered to be an effective approach to prevent obesity [3]. Brown adipose tissue (BAT) is one of the main thermogenic organs to maintain body temperature via energy expenditure.

Substantial literature has indicated that BAT is a very important tissue in the regulation of body weight. Increases in BAT thermogenesis may be an effective approach for obesity prevention [4, 5]. Interestingly, BAT thermogenesis, a typical type of adaptive thermogenesis, can be induced by cold exposure, which is mainly governed by the sympathetic nervous system in a hypothalamic neurons-dependent manner [6, 7]. Under cold-exposure conditions, hypothalamic nuclei, including the ventromedial hypothalamus, arcuate nucleus, dorsomedial hypothalamus, paraventricular hypothalamus, lateral hypothalamic areas, and the preoptic area (POA), coordinate to activate sympathetic nerves, leading to an increase in BAT thermogenesis to defend core body temperature in response to the reduction of ambient temperature [8]. Among these hypothalamic nuclei, the POA plays a crucial role in the regulation of BAT thermogenesis [9, 10]. In addition to thermoregulation, the POA also monitors body metabolic state and regulates food intake to maintain energy balance homeostasis [11, 12]. A previous report suggests that the antiobesity drug bupropion increases body temperature by acting on neural cells in the POA [13]. Thus, the POA has been recognized as an important brain area to maintain energy balance homeostasis [12], although intracellular signal cascades for thermoregulation are not fully understood.

p38, a stress-activated protein kinase, transduces signaling cascades to act on many biological processes or responses such as the inflammatory response, cell differentiation and proliferation, and glucose and lipid metabolism [14, 15]. There are four p38 family members: α, β, γ, and δ, which are activated via dual phosphorylation motif threonine-glycine-tyrosine in the activation loop by its upstream protein kinases. Activated p38 in turn phosphorylates and activates downstream substrates to transmit a signaling event [14]. p38α is most well characterized as a kinase and is widely expressed in multiple tissues [14]. Previous studies have shown that the p38α gene in adipocytes regulates adipogenesis and white adipocyte browning [16, 17]. In addition, in brown adipocytes, p38α transduces the cyclic AMP (cAMP) signaling cascade to promote BAT thermogenesis [18].

Despite a wealth of knowledge about the p38α functions on peripheral tissues, the action of p38α in the hypothalamus has not been fully explored. In this study, we find that the phosphorylation levels of mice hypothalamic proteins, in particular p38α, are dramatically altered by cold exposure. Ablation of p38α in the POA increases BAT thermogenesis, resulting in an attenuation of mice body weight gain. Our results suggest that p38α in the POA promotes obesity development, likely owing to a decrease in BAT thermogenesis.

METHODS

Animals

Mice were housed in groups of three to five animals per cage at room temperature with a 12-hour light/dark cycle, free access to water, and a standard chow diet. The housing condition for mice was grade specific-pathogen-free. Male C57BL/6J mice were purchased from Beijing Weitong Lihua Experimental Animal

Study Importance

What is already known?

- Brown adipose tissue (BAT) thermogenesis, a type of adaptive thermogenesis, can be triggered by cold exposure, which increases energy expenditure to prevent obesity development. The preoptic area (POA) in the hypothalamus is a crucial area in the regulation of BAT thermogenesis.

- In peripheral tissues, p38α is not only a transducer of stress and inflammation signals but it also performs important functions in the regulation of obesity and diabetes development.

What does this study add?

- Our study finds that numerous signaling pathways in the hypothalamus are modulated by acute cold exposure in the short term, in particular p38α, not extracellular signal-regulated kinase 1/2 (ERK1/2) and c-Jun NH2-terminal kinase (JNK), of the mitogen-activated protein kinase (MAPK) members.

- Our study demonstrates that deficiency of p38α in the POA protects against high-fat diet-induced body weight gain and improves insulin sensitivity and glucose tolerance, likely owing to an increase of BAT-mediated thermogenesis with unchanged food intake.

How might these results change the direction of research or the focus of clinical practice?

- Our results show a novel role of p38α in the central nervous system for thermoregulation and present a new intracellular signal cascade in the POA for regulation of BAT thermogenesis. p38α is also a potential target for the treatment of obesity in clinical practice in the future.

Technology Co. and used for experiments at the age of 12 weeks. p38α$^{flox/flox}$ mice were kindly provided by Lijian Hui [19]. p38α$^{flox/flox}$ mice were fed a high-fat diet (HFD) with 60% of kilocalories from fat (Research Diets, Inc., D12492) at 3 weeks after the adeno-associated virus 9 (AAV9) injection. Animal experiment protocols were approved by the ethics committee of Shandong Provincial Hospital affiliated with Shandong University in Jinan, China (No. 2018-006).

Mice were randomly assigned to each group. Small sample size (and smaller control group) was necessary to ensure 3R (replace, reduce, and refine) principles of animal testing. During the experiments, mice were monitored daily. Mice with significantly abnormal signs of inability to eat or drink, clinical symptomatology, toxicity, or unresponsiveness were recorded, and the data from these mice were

excluded from statistical analysis. Body weight of mice was measured weekly at a fixed time (from 9 AM to 10 AM) using a weighing balance. The percentage of body weight gain was calculated as follows: (body weight on specific week [grams] − initial body weight)/initial body weight × 100.

Cold exposure and temperature measurement

Male mice were exposed to 4 °C for 4 hours, and then the hypothalamus was dissected for proteomic and protein phosphorylation assays. At the fifth week after virus injection, mice with p38α over-expression were exposed to 10 °C environments for 3 hours in a single cage, and rectal and interscapular temperature was measured at 0, 30, 60, 120, and 180 minutes. Rectal and interscapular temperature of p38α$^{POA-/-}$ mice was measured at room temperature between 9 AM and 11 AM during the fourth and fifth weeks after virus injection. The specific measurement methods are described in the online Supporting Information.

Metabolic analysis

Energy expenditure, oxygen consumption, carbon dioxide production, locomotor activity, and respiratory exchange ratio of mice were measured by Oxymax system (Columbus Instruments Comprehensive Lab
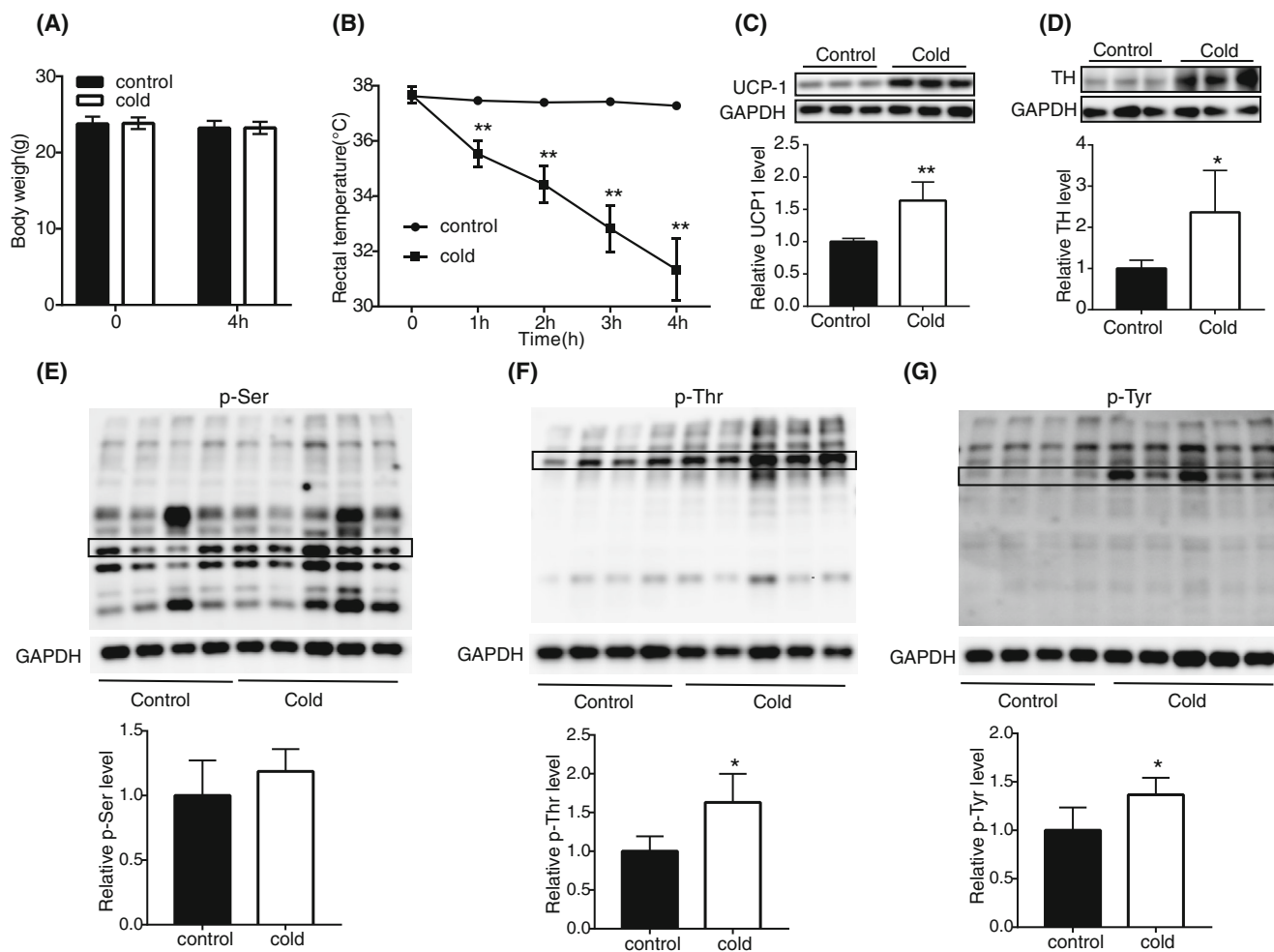

FIGURE 1 Hypothalamus protein phosphorylation with acute cold exposure. (A) Body weight of control ($n = 5$) and cold-exposed ($n = 5$) mice before and after cold exposure. (B) Rectal temperature of control ($n = 5$) and cold-exposed ($n = 5$) mice. (C) UCP1 protein levels were determined by immunoblot analysis of BAT lysates from control and cold-exposed mice. (D) TH protein levels were determined by immunoblot analysis of BAT lysates of control and cold-exposed mice. (E) Pan-phosphoserine levels of total proteins were determined by immunoblot analysis of hypothalamus lysates of control and cold-exposed mice. Quantified analysis of representative bands (boxed in black). (F) Pan-phosphothreonine levels of total proteins were determined by immunoblot analysis of hypothalamus lysates of control and cold-exposed mice. Quantified analysis of representative bands (boxed in black). (G) Pan-phosphotyrosine levels of total proteins were determined by immunoblot analysis of hypothalamus lysates of control and cold-exposed mice. Quantified analysis of representative bands (boxed in black). Data are represented as mean ± SD; *$p < 0.05$, **$p < 0.01$. Data in panel B were analyzed using two-way repeated measurements ANOVA. Each lane represents one mouse. BAT, brown adipose tissue; TH, tyrosine hydroxylase; UCP1, uncoupling protein 1

Animal Monitoring System [CLAMS]) at week 6 after virus injection. One mouse was excluded from indirect calorimetry because of leakage air in its metabolic chamber. The food weight was manually quantified before and after indirect calorimetry measurement, and then the differential food weight was recorded as the total food intake. Body composition of mice was measured *in vivo* by a minispec body composition analyzer (Bruker Minispec LF90II) after indirect calorimetry measurement.
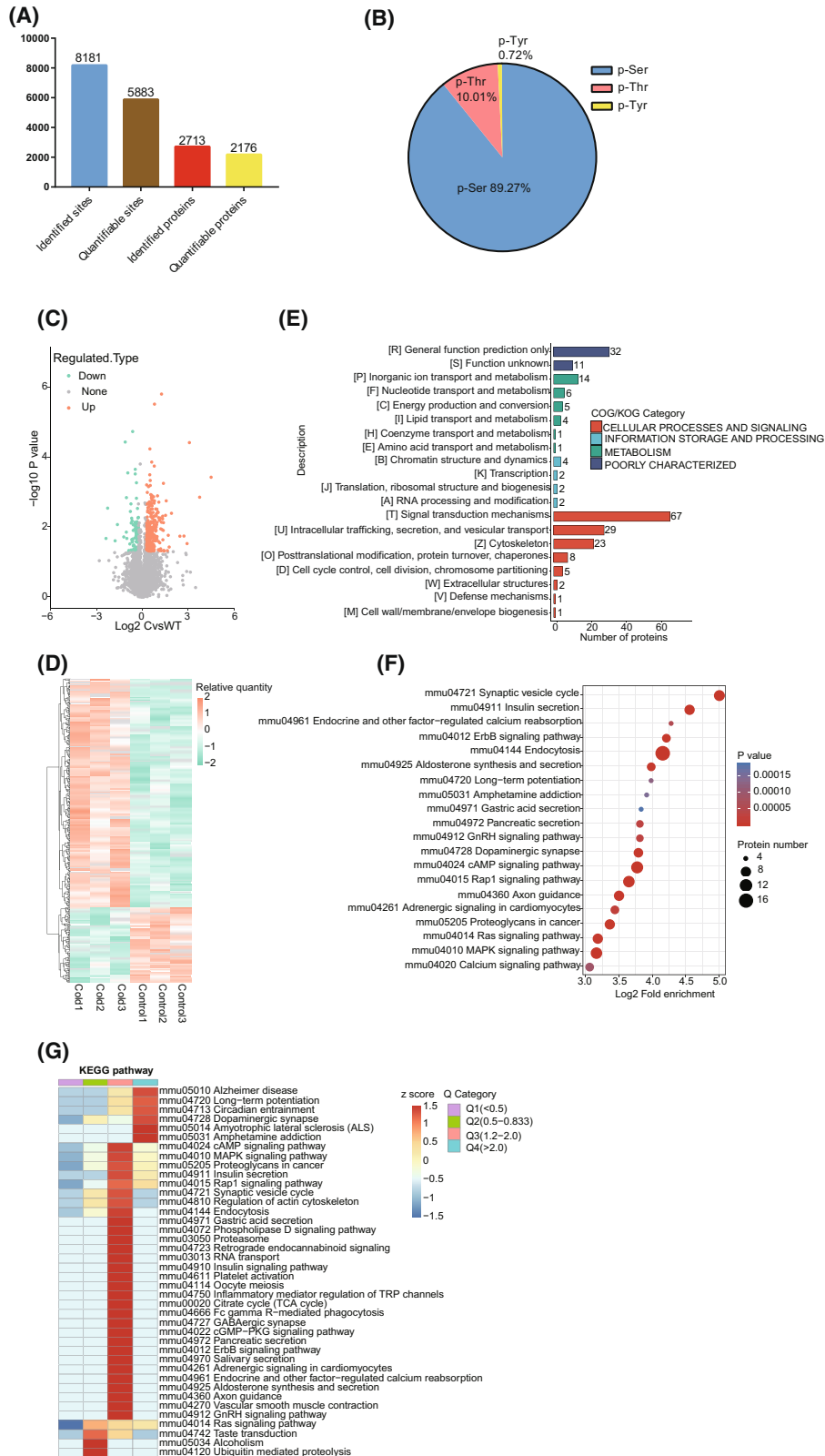

FIGURE 2 Legend on next page.

Glucose tolerance tests and insulin tolerance tests

Glucose tolerance tests and insulin tolerance tests were performed by intraperitoneal injection of 2 g/kg of glucose to mice after overnight fasting or 0.75 U/kg of insulin to mice after 4 hours of fasting, respectively. Blood glucose from tail vein was measured at 0, 30, 60, 90, and 120 minutes with a glucose meter (Roche). Blood glucose values outside the measurement range were excluded.

Viruses and stereotaxic surgeries

p38α$^{flox/flox}$ mice or wild-type mice were placed on a stereotaxic alignment system (1900, David Kopf Instruments), and anesthetization by 2% isoflurane was maintained during surgeries. For the deletion of p38α in the POA, p38α$^{flox/flox}$ mice were injected with pAAV9-CAG-EGFP-P2A-Cre-WPRE (AAV9-green fluorescent protein [GFP]-Cre, 5.0×10^{12} viral genomes [vg]/mL) or pAAV9-CAG-EGFP-P2A-WPRE (AAV9-GFP, 5.0×10^{12} vg/mL) bilaterally into the POA (anteroposterior: $+0.14$ mm, mediolateral: ±0.3 mm, dorsoventral: -5.6 mm; 1 uL in each side at 0.1 uL/min). AAV viruses were purchased from Obio Technology. For the overexpression of p38α in the POA, wild-type mice were injected with the AAV9-p38α or AAV9-control virus and AAV9-Cre-GFP virus together bilaterally into the POA. The p38α gene was inserted into a pAAV9-CMV-bGlobin-FLEX-MCS-EGFP-WPRE-hGH-polyA vector (AAV9-p38α, 1.0×10^{12} vg/mL). The empty control vector was pAAV9-CMV-bGlobin-FLEX-MCS-EGFP-WPRE-hGH-polyA vector (AAV9-control, 1.0×10^{12} vg/mL). These viruses were generated and purified by Genechem Co., Ltd. Injection sites were verified by GFP fluorescence. Mice with injection sites not in the POA were excluded, and only those animals with injection sites correctly in the POA were included in the study.

Label-free quantitative proteomics and bioinformatics analysis

The experimental procedures for proteomics analysis included protein preparation, trypsin digestion, affinity enrichment, liquid chromatography with tandem mass spectrometry (LC–MS/MS) analysis, and database search. The proteomics experiments and subsequent bioinformatics analysis in our research were supported by Jingjie PTM BioLabs. Ingenuity Pathway Analysis (IPA; QIAGEN) was used to analyze upstream regulatory molecules and regulator effects networks [20]. The details are provided in the online Supporting Information.

Histological analysis of tissues

Paraformaldehyde-fixed, paraffin-embedded sections of liver, BAT, and white adipose tissue (WAT) were stained with hematoxylin-eosin (H&E) for histology. Paraffin-embedded brain sections were incubated with p38α antibody (1:200, AF8691, R&D Systems) and visualized with the 3,3'-diaminobenzidine (DAB) chromogen kit (DAB kit, Zhongshan Golden Bridge Biotechnology Co. Ltd). Images were acquired by TissueFAXS PLUS (Meyer Instruments, Inc.). The details are provided in the online Supporting Information.

Immunoblotting

Fat and hypothalamus tissues were lysed in radioimmunoprecipitation assay buffer (Shenergy Biocolor Bioscience & Technology Co.) containing protease inhibitors and phosphatase inhibitors. Tissue lysates were immunoblotted with antibodies: anti-uncoupling protein-1 (UCP1; 1:5000, ab209483, Abcam), anti-tyrosine hydroxylase (TH; 1:1000, ab112, Abcam), anti-phospho-p38 (p-p38; 1:1000, 4511, Cell Signaling Technology, Inc.), anti-p38 (1:1000, AF8691, R&D Systems), anti-phospho-extracellular signal-regulated kinase (p-ERK; 1:1000, 4376, Cell Signaling Technology), anti-ERK (1:1000, 4695, Cell Signaling Technology), anti-phospho-c-Jun NH2-terminal kinase (p-JNK; 1:1000, 9255, Cell Signaling Technology), anti-JNK (1:1000, 9252, Cell Signaling Technology), anti-phosphoserine (1:1000, sc-81,514, Santa Cruz Biotechnology, Inc.), anti-phosphothreonine (1:1000, 705RM, Jingjie PTM BioLabs), anti-phosphotyrosine (1:1000, 702RM, Jingjie PTM BioLabs),

FIGURE 2 Phosphoproteomics analysis of hypothalamus after cold exposure. (A) Number of identified phosphorylation sites and phosphoproteins. (B) Percentages of phosphoserines, phosphothreonines, and phosphotyrosines. (C) Volcano plot shows the phosphorylation site statistical significance (on the y-axis) over the log2-fold change after normal shrinkage (on the x-axis) for all the samples from differential expression analysis. Each point represents a phosphorylation site, with orange and green points representing significantly up- and downregulated phosphorylation sites, respectively, and gray points indicating no significant change. (D) Heat map analysis of differential phosphosites profiles among the six samples tested. The rows display phosphorylation site, and the columns show the different samples. (E) COG/KOG functional classification distribution maps of proteins corresponding to differential phosphorylation site. The y-axis represents the number of proteins, and the x-axis represents the COG/KOG categories. (F) KEGG enrichment analysis of the differential phosphorylated proteins. The bubble size reflects the number of differentially enriched proteins, and the bubble color represents the p value of the enrichment significance. (G) Heat map of the clustering analysis of KEGG enrichment for the differentially phosphorylated proteins. Category Q represents differential modification folds: Q1 (<0.5); Q2 (0.5-0.833); Q3 (1.2-2.0); and Q4 (>2.0). The p value was performed logarithmic transformation of -log10 to achieve data matrix. Z transformation was used in the data matrix of p value for the hierarchical clustering analysis. Red indicates high enrichment level; blue indicates low enrichment level. A two-tailed Fisher exact test was employed to test the enrichment of the identified modified proteins against all proteins in the species database. Corrected $p < 0.05$ was considered significant. COG, Clusters of Orthologous Groups; KEGG, Kyoto Encyclopedia of Genes and Genomes; KOG, eukaryotic clusters [Color figure can be viewed at wileyonlinelibrary.com]
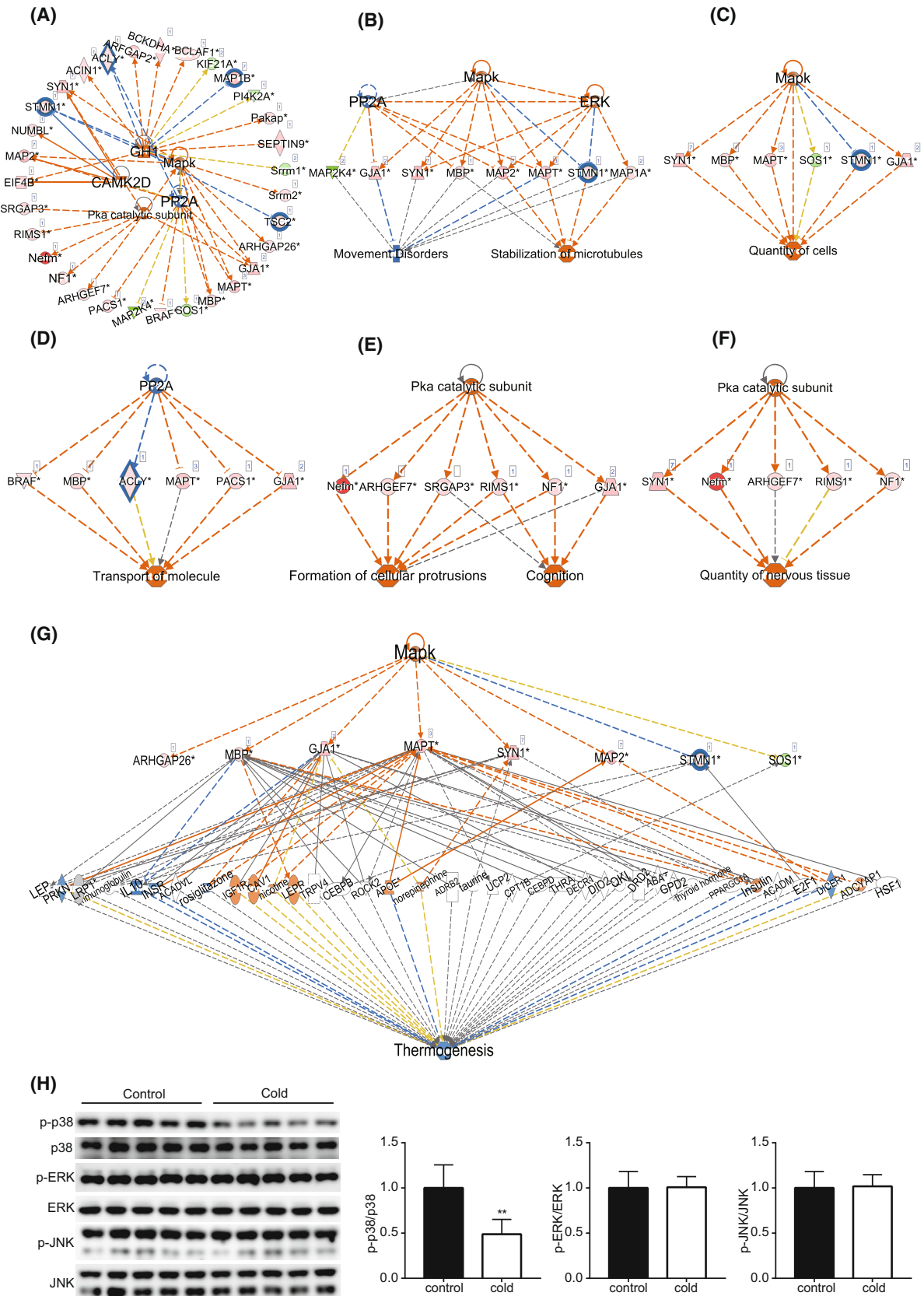
FIGURE 3 Legend on next page.

anti-Cre (1:1000, 15036, Cell Signaling Technology), anti-GFP (1:1000, ab6673, Abcam), glyceraldehyde-3-phosphate dehydrogenase (GAPDH; 1:7500, 60,004-1-Ig, Proteintech), and heat shock protein 90 (Hsp90; 1:5000, 13,171-1-ap, Proteintech). The signals were detected by Amersham Imager 680. Protein band intensities were analyzed using PhotoShop software (Adobe, Inc.).

Statistical analysis

Data were expressed as means ± standard deviation (SD). Energy expenditure was analyzed by ANCOVA with body weight as covariate in accordance with published methods [21]. Two-way repeated measurements ANOVA (normally distributed data) or Scheirer-Ray-Hare test (not normally distributed data) was used to analyze sequential measurements. $P < 0.05$ was considered statistically significant. ANCOVA was performed with SPSS Statistics version 22.0 (IBM Corp.), and the Scheirer-Ray-Hare test was performed with R software (R version 4.1.2, R Foundation), whereas other experimental data were analyzed by two-tailed Student t test with Prism 7.0 (GraphPad Software Inc.).

RESULTS

Cold exposure alters the phosphorylation profile of hypothalamic proteins

It has been previously shown that cold exposure promotes BAT thermogenesis dependent upon the hypothalamic signals; however, the underlying intracellular signal cascades in the hypothalamus are not fully understood. To probe these signaling pathways in hypothalamic neurons for regulation of BAT thermogenesis, we performed a cold-exposed assay in a mice model. After cold exposure, there was no significant difference in mice body weight (Figure 1A). In contrast, the rectal temperature of mice with cold exposure significantly decreased compared with that of mice with control ambient temperature (Figure 1B). Consistently, the protein level of UCP1, a marker of BAT thermogenesis, and the protein level of TH, a marker of sympathetic

innervation, were dramatically increased in BAT after cold exposure (cold-exposed mice vs. control mice, for UCP1: 1.64 ± 0.29 vs. 1.00 ± 0.05, $p < 0.05$; for TH: 2.36 ± 1.01 vs. 1.00 ± 0.20, $p < 0.05$; Figure 1C,D), which demonstrates that cold exposure indeed augmented sympathetic drive and BAT thermogenesis.

Because protein phosphorylation/dephosphorylation is the most common mechanism of transmitting signals throughout the cell to regulate many cellular processes [22], we first examined the total protein phosphorylation levels in the hypothalamus with or without cold exposure. Protein phosphorylation levels were recognized by anti-pan-phosphoserine, -phosphothreonine, and -phosphotyrosine antibodies. Immunoblotting results showed that the phosphorylation levels of protein residues threonine and tyrosine were significantly changed (cold-exposed mice vs. control mice, for phosphothreonine: 1.63 ± 0.37 vs. 1.00 ± 0.19, $p < 0.05$; for phosphotyrosine: 1.37 ± 0.18 vs. 1.00 ± 0.24, $p < 0.05$; Figure 1E,G), which indicates that numerous signal cascades are triggered in the hypothalamus.

Multiple hypothalamic signaling pathways are activated by cold exposure

To disclose these hypothalamic signaling pathways involved in the regulation of BAT thermogenesis, we used an optimized phosphoproteomic workflow based on label-free quantitation to determine protein phosphorylation levels from the hypothalamus of six mice with or without cold exposure. The phosphoproteomic workflow identified 8181 phosphorylation sites covering 2713 phosphoproteins, of which 5883 phosphorylation sites on 2176 proteins were identified (Figure 2A). Analysis of the phosphorylated amino acid distribution showed that 89.27% of phosphorylation sites were on serine, 10.01% of phosphorylation sites were on threonine, and 0.72% of the total phosphorylation sites belonged to tyrosine-containing peptides (Figure 2B). Using 1.2-fold changes as the threshold for differentially modified phosphorylation sites, we identified 377 phosphorylation sites mapped to 285 upregulated or downregulated differentially phosphorylated proteins (DPPs), specifically 281 upregulated phosphorylation sites and 96 downregulated phosphorylation sites (Figure 2C,D). According to differential phosphorylation sites, Clusters of Orthologous Groups (COG) annotation grouped the

FIGURE 3 Hypothalamic MAPK signaling pathways are associated with cold exposure. (A) IPA Upstream Regulator Analysis of DPPs. The upstream regulators, including MAPK, PP2A, PKA, CAMK2D, and GH1, were predicted to be responsible for the DPPs. Downstream biological functions analysis of different DPPs combined with predicted upstream regulators by IPA Regulator Effects analysis tool. (B,C) Three upstream regulators, MAPK, PP2A, and ERK, were combined with different DPPs to analyze downstream effects. (D) PP2A was combined with DPPs to analyze downstream effects. (E,F) PKA catalytic subunit was combined with different DPPs to analyze downstream effects. (G) IPA regulatory network analysis of DDPs regulated by MAPK and thermogenesis. In the network nodes, the upper panel is the upstream regulator (MAPK) of the DPPs in the second panel, the third panel is intermediate proteins between DPPs and thermogenesis, and the lower panel shows the biological functions-thermogenesis. (H) Expression levels of MAPK (ERK1/2, p38 MAPK, and JNK) pathways were determined by immunoblot analysis of hypothalamus lysates from control and cold-exposed mice. Data are represented as mean ± SD; *$p < 0.05$, **$p < 0.01$. Each lane represents one mouse. For the network edges, a solid line indicates direct interaction, whereas a dashed line indicates indirect interaction. Node colors: orange = activation; blue = inhibition; green = downregulation; red = upregulation. Z score algorithm was used to make predictions. Z score >2 was considered to be activated, and z score < −2 was considered to be inhibited. CAMK2D, calcium/calmodulin dependent protein kinase II delta; DPP, differentially phosphorylated protein; GH1, growth hormone 1; IPA, Ingenuity Pathway Analysis; PP2A, protein phosphatase 2 [Color figure can be viewed at wileyonlinelibrary.com]

DPPs into four major functional categories: 1) cellular processes and signaling; 2) information storage and processing; 3) metabolism; and 4) poorly characterized (Figure 2E). Notably, the largest number of phosphorylated proteins were classified into the "signal transduction mechanisms" (67 proteins) term (Figure 2E), indicating that numerous signal transduction events were triggered in the hypothalamus by cold exposure. Consistently, subsequent Kyoto Encyclopedia of Genes and Genomes (KEGG) pathway analysis of these DPPs enriched the predominant ErbB, gonadotropin-releasing hormone 1 (GnRH), cAMP, Rap1, mitogen-activated protein kinase (MAPK), Ras, and Ca^{2+} signaling pathways (Figure 2F). Then we divided differential phosphorylation sites into

four groups (quartiles) according to the phosphorylation level fold change (Q): Q1 (<0.5, proteins downregulated more than 2-fold); Q2 (0.5-0.833, proteins downregulated 1.2- to 2-fold); Q3 (1.2-2.0, proteins upregulated 1.2- to 2-fold); Q4 (>2.0, proteins upregulated more than 2-fold). According to Q value, cluster analysis of KEGG enrichment was performed to figure out the potential connections and differences in KEGG pathways among different groups. As shown in Figure 2G, cAMP, MAPK, Rap1, insulin, protein kinase G (PKG), ErbB, and GnRH signaling pathways were highly enriched in the Q3 (1.2-2.0) category. Thus, these results show that multiple signaling cascades in the hypothalamus are dramatically triggered in response to cold stimulation.
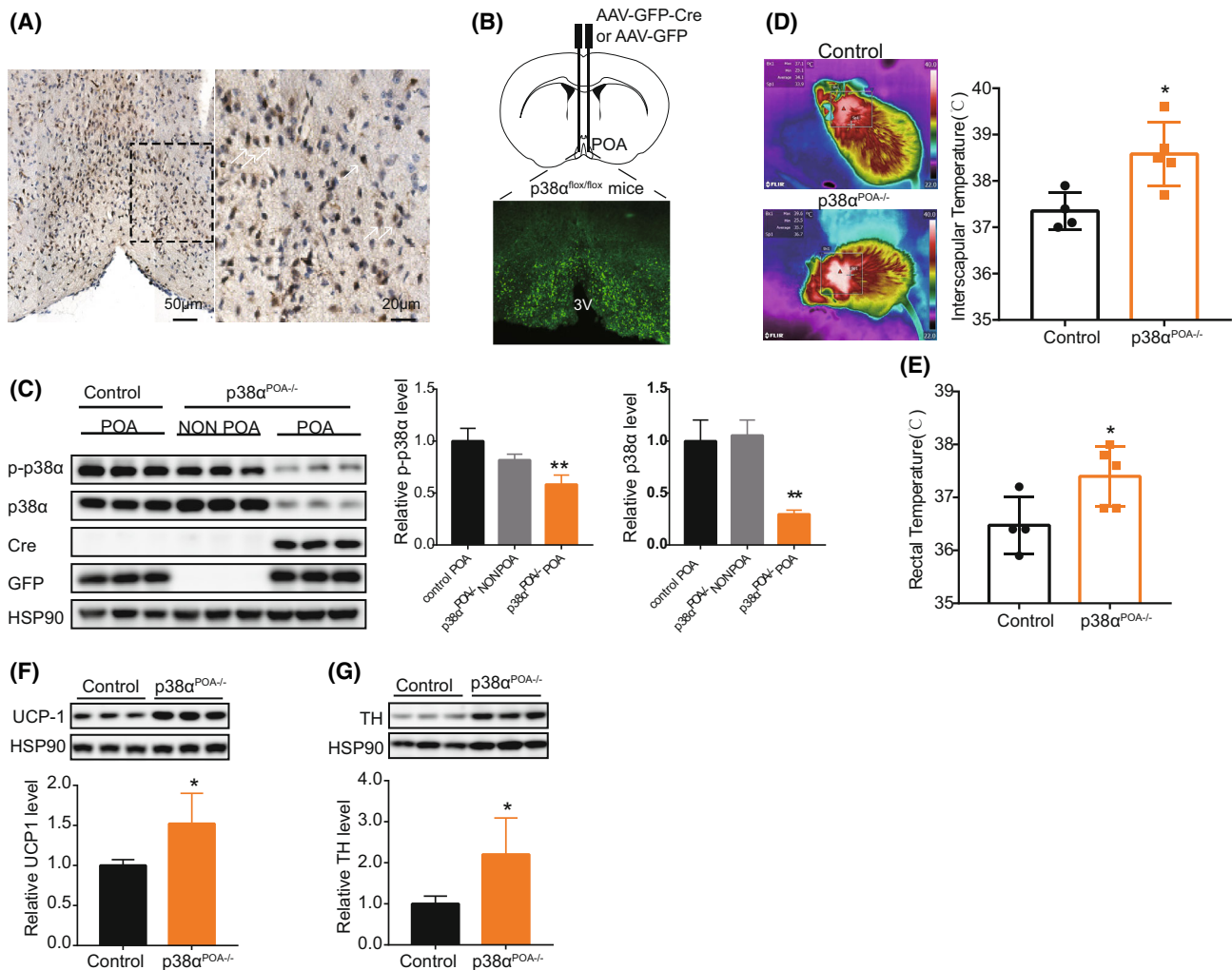

FIGURE 4 p38α deficiency in the POA increases BAT thermogenesis. (A) Representative immunohistochemistry of p38α in the POA. Arrows represents p38α-positive cells. Scale bars: 50 μm (low magnification); 20 μm (high magnification). (B) Schematic of the AAV9 stereotaxic injection to the POA of p38α^flox/flox mice and representative image. Scale bar: 500 μm. (C) The p38α and p-p38α levels were examined by immunoblotting. (D) Representative infrared thermal images and interscapular temperature in the BAT of control ($n = 4$) and p38α^POA−/− ($n = 5$) mice at room temperature. (E) Rectal temperature of control ($n = 4$) and p38α^POA−/− ($n = 5$) mice at room temperature. (F) UCP1 protein levels in BAT of control and p38α^POA−/− mice. (G) TH protein levels in BAT of control and p38α^POA−/− mice. Control mice with AAV9-GFP virus injection. p38α^POA−/− mice with AAV9-GFP-Cre virus injection. Data are represented as mean ± SD; *$p < 0.05$, **$p < 0.01$. AAV9, adeno-associated virus 9; BAT, brown adipose tissue; GFP, green fluorescent protein; POA, preoptic area; TH, tyrosine hydroxylase; UCP1, uncoupling protein 1 [Color figure can be viewed at wileyonlinelibrary.com]

Hypothalamic MAPK signaling pathway is associated with thermogenesis

Because numerous hypothalamic signaling pathways are associated with cold exposure, we next used the IPA tool to identify the most significant pathways for thermoregulation. Upstream regulators of the 285 DPPs were identified through IPA Upstream Regulator Analysis. Growth hormone protein 1 (GH1), calcium/calmodulin dependent protein kinase II delta (CAMK2D), cAMP-dependent protein kinase (PKA) catalytic subunit, MAPK, and protein phosphatase 2 (PP2A) were predicted and enriched as upstream modulators of DPPs (Figure 3A). Next, we analyzed the biological functions and signaling cascades of these predicted upstream modulators (GH1, CAMK2D, PKA catalytic subunit, MAPK, and PP2A) by the IPA Regulator Effects tool. MAPK, PP2A, and PKA were directly associated with quantity of cells, movement disorders, stabilization of microtubules, transport of molecule, formation of cellular protrusions, and cognition (Figure 3B,F).

Strikingly, we analyzed both upstream modulators (GH1, CAMK2D, PKA catalytic subunit, MAPK, and PP2A) and KEGG data of signaling pathways (ErbB, GnRH, cAMP, Rap1, MAPK, insulin, PKG, Ras, and Ca^{2+}; Figure 2F,G) together, and the MAPK pathway was the only one presented in both results, suggesting that MAPK signals are likely one of the most significantly affected signaling cascades by cold exposure. To test this, we further analyzed the linkage between MAPK downstream DPPs and thermogenesis/thermoregulation. Indeed, the DPPs (myelin basic protein [MBP], gap junction alpha-1 protein [GJA1], microtubule-associated protein tau [MAPT], synapsin 1 [SYN1], microtubule-associated protein 2 [MAP2], stathmin [STMN1], and son of sevenless homolog 1 [SOS1]), regulated by MAPK, tightly connect to thermogenesis via numerous downstream intermediate molecules (Figure 3G).

To verify whether the MAPK signaling pathway in the hypothalamus is involved in the regulation of thermoregulation, we first examined the phosphorylation levels of the MAPK members,
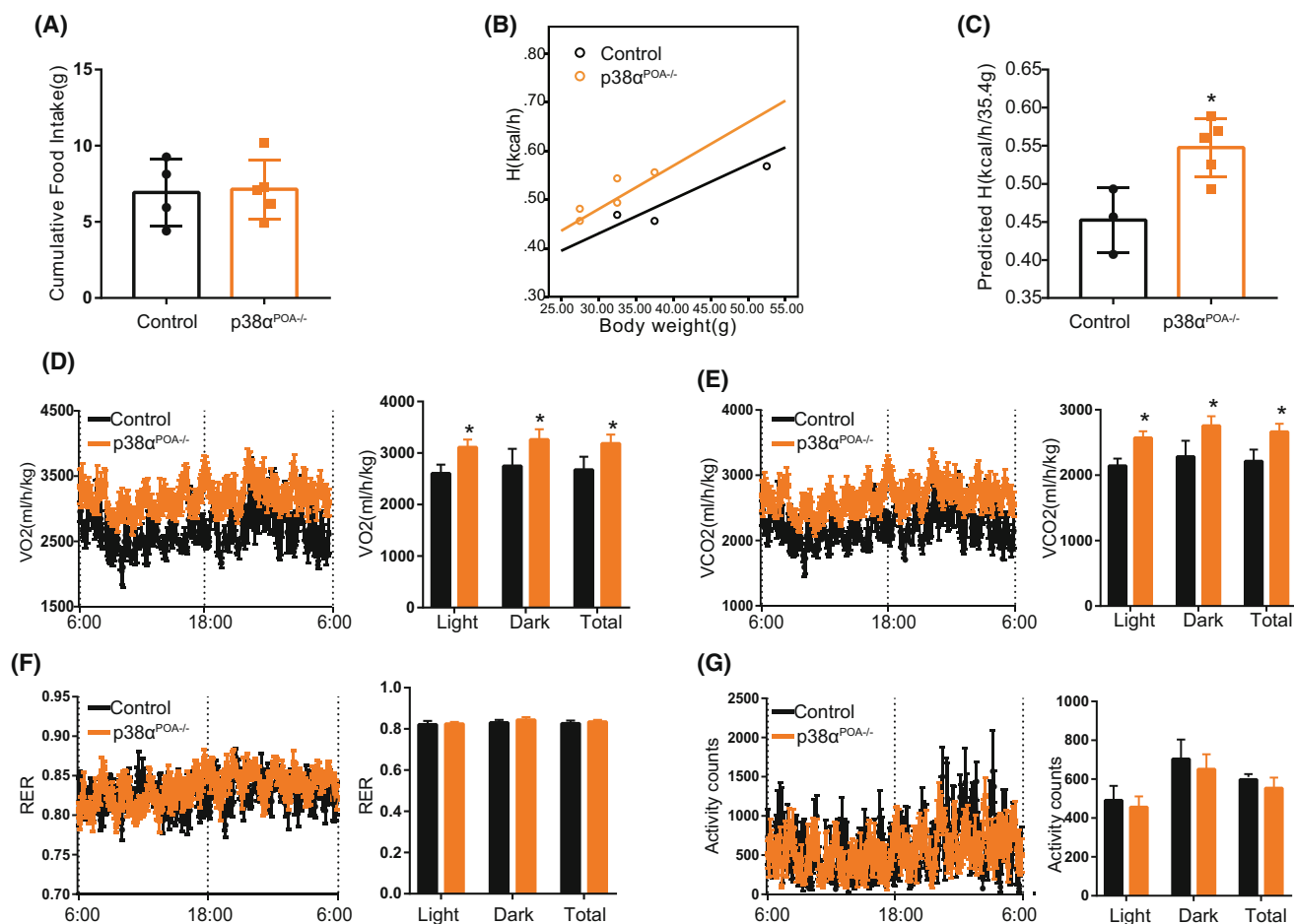

FIGURE 5 p38α deficiency in the POA increases energy expenditure. (A) Cumulative food intake for 3 days of control ($n = 4$) and p38α$^{POA-/-}$ ($n = 5$) mice. (B) Energy expenditure of control ($n = 3$) and p38α$^{POA-/-}$ ($n = 5$) mice. Energy expenditure was analyzed by ANCOVA with body weight as covariate. (C) ANCOVA predicted energy expenditure of control ($n = 3$) and p38α$^{POA-/-}$ ($n = 5$) mice at a given body mass of 35.4 g. (D) Oxygen consumption of control ($n = 3$) and p38α$^{POA-/-}$ ($n = 5$) mice. (E) Carbon dioxide production of control ($n = 3$) and p38α$^{POA-/-}$ ($n = 5$) mice. (F) Respiratory exchange ratio (RER) of control ($n = 3$) and p38α$^{POA-/-}$ ($n = 5$) mice. (G) Locomotor activity of control ($n = 3$) and p38α$^{POA-/-}$ ($n = 5$) mice. Control mice with AAV9-GFP virus injection. p38α$^{POA-/-}$ mice with AAV9-GFP-Cre virus injection. Data are represented as mean $\pm$ SD; *$p < 0.05$. AAV9, adeno-associated virus 9; GFP, green fluorescent protein; POA, preoptic area [Color figure can be viewed at wileyonlinelibrary.com]

including ERK1/2, p38α, and JNK, after cold exposure. The phosphorylated p38α level in the hypothalamus was significantly decreased in cold-exposed mice (cold-exposed mice vs. controls mice: 2.66 ± 0.89 vs. 5.44 ± 1.39, $p < 0.05$; Figure 3H). Notably, no dramatic changes in the phosphorylation levels of ERK1/2 and JNK were observed after cold exposure (Figure 3H). These results suggest that p38α signaling in the hypothalamus is strongly associated with thermoregulation.

p38α deficiency in the POA promotes BAT thermogenesis

Because the POA is a critical hypothalamic area for thermoregulation [9, 10], we first examined the expression of p38α protein in the POA by immunohistochemical staining. p38α protein was widely detected in the POA (Figure 4A). To determine the role of p38α in the POA, we next generated a mouse line (p38α^POA−/−) by ablating p38α in the

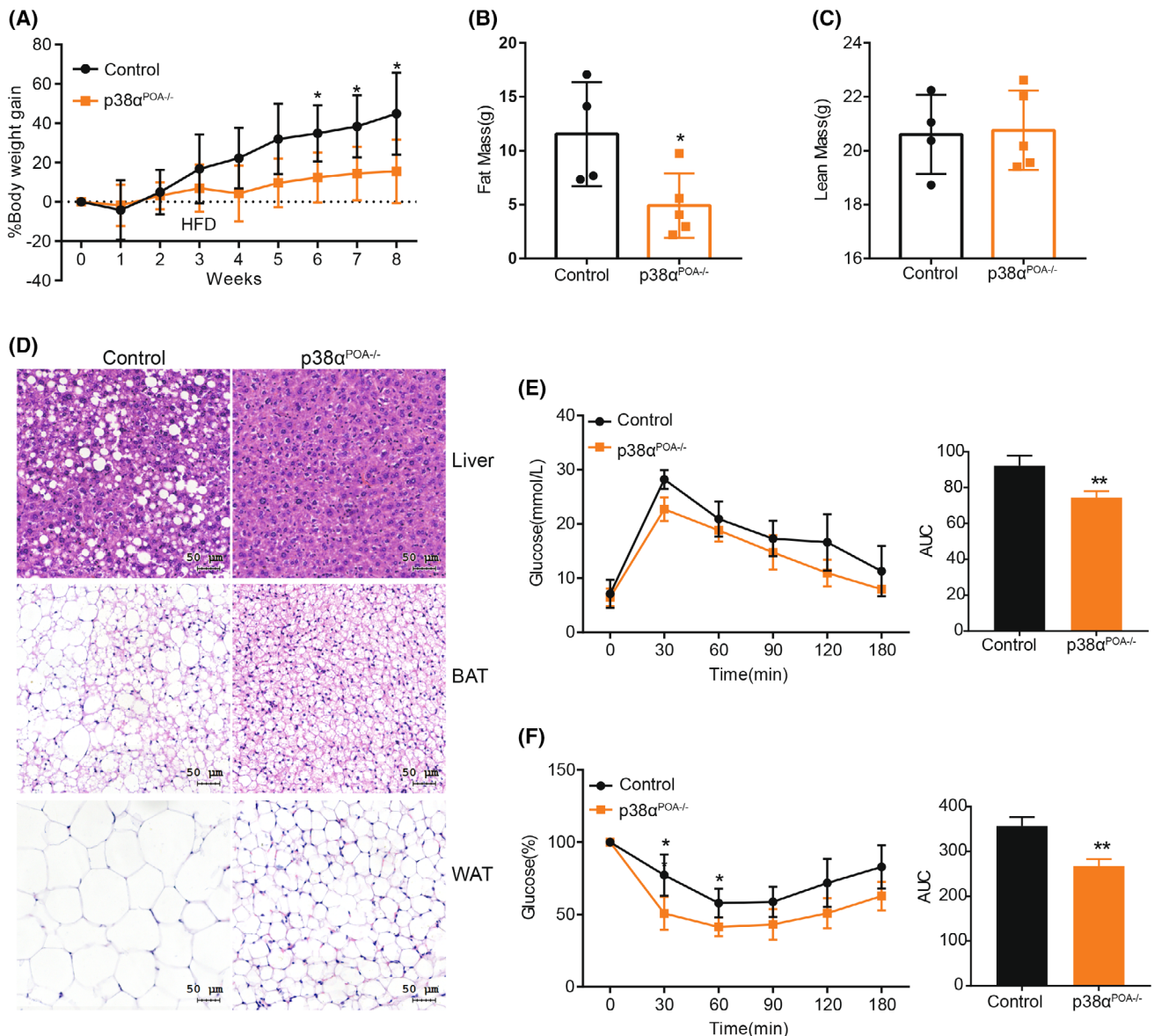**FIGURE 6** p38α deficiency in the POA protects against diet-induced obesity. (A) Body weight gain curve of control ($n = 4$) and p38α^POA−/− ($n = 5$) mice. A high-fat diet was supplied to mice from 3 weeks after the virus injection. (B) Fat mass of control ($n = 4$) and p38α^POA−/− ($n = 5$) mice. (C) Lean mass of control ($n = 4$) and p38α^POA−/− ($n = 5$) mice. (D) Representative pictures of liver, BAT, and WAT H&E staining. (E) Glucose tolerance test of control ($n = 4$) and p38α^POA−/− ($n = 5$) mice. (F) Insulin tolerance test of control ($n = 4$) and p38α^POA−/− ($n = 5$) mice. Control mice with AAV9-GFP virus injection. p38α^POA−/− mice with AAV9-GFP-Cre virus injection. Data are represented as mean $\pm$ SD; *$p < 0.05$, **$p < 0.01$. Data in panel A were analyzed using Scheirer-Ray-Hare test; data in panels E and F were analyzed using two-way repeated measurements ANOVA. AAV9, adeno-associated virus 9; BAT, brown adipose tissue; GFP, green fluorescent protein; POA, preoptic area; WAT, white adipose tissue [Color figure can be viewed at wileyonlinelibrary.com]

POA via expressing AAV9-Cre-GFP virus in the POA of p38α$^{flox/flox}$ mice (Figure 4B) [17, 19, 23]. The efficacy and localization of the Cre gene expression in the POA were revealed by GFP florescence and p38α immunoblotting (Figures 4B,C and Supporting Information Figure S1). Importantly, p38α$^{POA-/-}$ mice exhibited an elevated interscapular BAT and rectal temperature compared with the control mice (38.58 ± 0.68 vs. 37.35 ± 0.40, $p < 0.05$ and 37.4 ± 0.57 vs. 36.48 ± 0.54, $p < 0.05$, respectively; Figure 4D,E). Consistently, UCP1 and TH protein levels in BAT of p38α$^{POA-/-}$ mice were also higher than those of controls (1.52 ± 0.38 vs. 1.00 ± 0.07, $p < 0.05$ and 2.21 ± 0.88 vs. 1.00 ± 0.19, $p < 0.05$, respectively; Figure 4F,G). Thus, these results elucidate that p38α in the POA is involved in the regulation of BAT thermogenesis.

p38α deficiency in the POA enhances energy expenditure

p38α deletion in the POA increased the BAT thermogenesis, resulting in an elevation in BAT temperature, which suggests an altered energy balance status in p38α$^{POA-/-}$ mice. To clarify this issue, we monitored food intake and energy expenditure in p38α$^{POA-/-}$ mice. p38α$^{POA-/-}$ mice showed no dramatic change of food consumption

compared with the controls when fed with an HFD (Figure 5A). However, a significant increase in energy expenditure was observed in p38α$^{POA-/-}$ mice (Figure 5B,C), as revealed by oxygen consumption (Figure 5D) and carbon dioxide production (Figure 5E). Notably, there were no obvious differences in respiratory exchange ratio (Figure 5F) and locomotor activity (Figure 5G) among p38α$^{POA-/-}$ and control mice. Therefore, p38α deletion in the POA increases BAT thermogenesis, resulting in an increase in whole-body energy expenditure.

p38α deficiency in the POA attenuates obesity development

As described earlier, lacking p38α in the POA increased whole-body energy expenditure, at least in part owing to an increase in BAT thermogenesis. Next, we asked whether p38α in the POA also regulates obesity development and metabolic disorders. To address this issue, we fed p38α$^{POA-/-}$ and control mice with an HFD for another 5 weeks. p38α$^{POA-/-}$ mice on an HFD exhibited significantly attenuated body weight gain (Figure 6A) and fat mass (adiposity) compared with control mice (4.92 ± 2.99 vs. 11.55 ± 4.83, $p < 0.05$; Figure 6B and Supporting Information Figure S2A), whereas, for lean mass, there
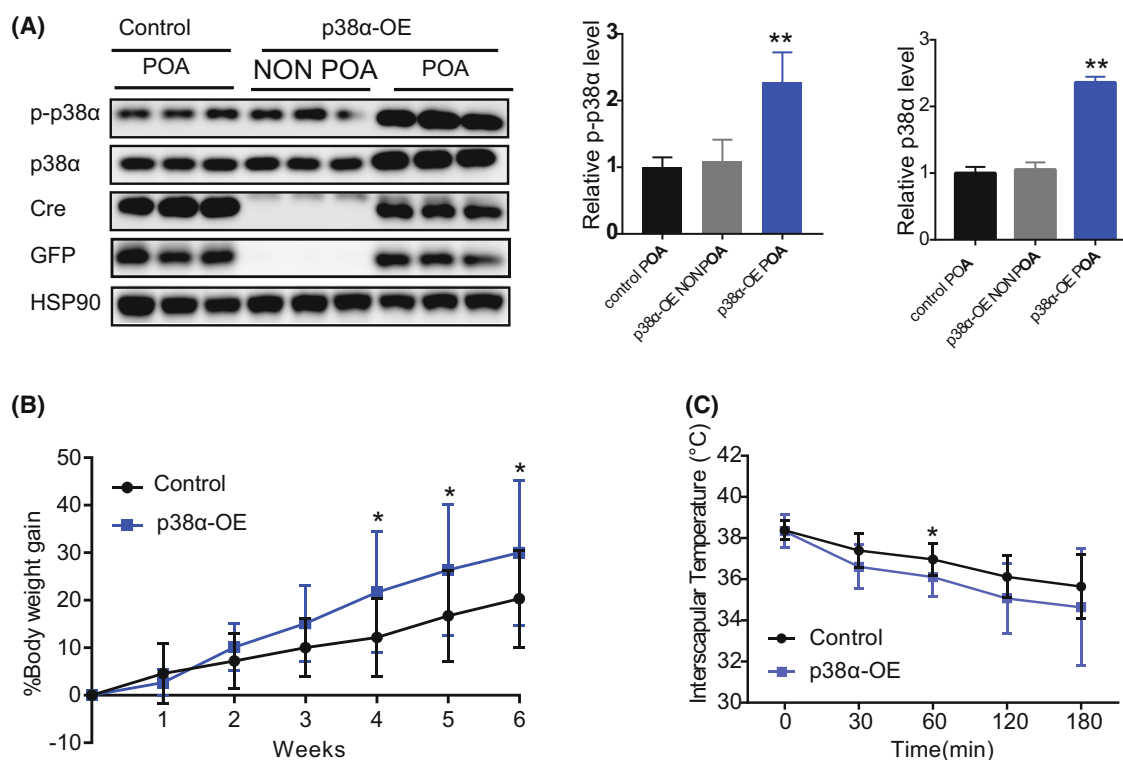

FIGURE 7 p38α overexpression in the POA increases body weight gain. (A) p38α and p-p38α levels were examined by immunoblotting. (B) Body weight gain curve of control ($n = 16$) and p38α-OE ($n = 14$) mice. (C) Interscapular temperature in the brown adipose tissue of control ($n = 15$) and p38α-OE ($n = 13$) mice under cold exposure. Control mice with AAV9-control virus injection. p38α-OE mice with AAV9-p38α virus injection. Data are represented as mean ± SD; *$p < 0.05$, **$p < 0.01$. Data in panel B were analyzed using two-way repeated measurements ANOVA; data in panel C were analyzed using Scheirer-Ray-Hare test. AAV9, adeno-associated virus 9; OE, overexpression; POA, preoptic area; GFP, green fluorescent protein [Color figure can be viewed at wileyonlinelibrary.com]

was no obvious difference among p38α$^{POA-/-}$ and control mice (Figure 6C and Supporting Information Figure S2B). Consistently, p38α$^{POA-/-}$ mice had smaller adipocyte sizes and fewer fat droplets in liver than control mice (Figure 6D), accompanied by improved glucose tolerance and insulin sensitivity (Figure 6E,F). In contrast, overexpression of p38α in the POA by stereotaxic injection of AAV9-p38α or AAV9-control and AAV9-Cre-GFP virus together (Figure 7A and Supporting Information Figure S3) led to an increase of body weight gain (Figure 7B). Notably, mice with overexpression of p38α displayed dramatic reduction of interscapular BAT temperature compared with control mice under cold-exposure conditions (Figure 7C). Thus, all of these data demonstrate that p38α in the POA modulates obesity development and metabolism via regulation of BAT thermogenesis.

DISCUSSION

Enhancement of energy expenditure via promotion of BAT thermogenesis is considered as one of the most effective approaches to prevent obesity development. Although the central nervous system performs a crucially important role in the control of BAT thermogenesis, what remains to be completely understood is these intracellular signaling cascades that underlie the central thermoregulation. In this study, p38α deficiency in the POA attenuated the development of obesity and metabolic disorders, which unmasks a crucial regulatory role of p38α in BAT thermogenesis.

Cold exposure has been widely recognized as a potential way for treatment of obesity via elevation of UCP1-mediated non-shivering BAT thermogenesis, leading to increase of energy expenditure [6]. Cold-induced BAT thermogenesis depends on the hypothalamus-activated BAT sympathetic nerve activity. In particular, the POA in the hypothalamus is a critical area for neural thermoregulation [8, 10]. However, it is unclear which intracellular signaling cascades in the POA are required for the regulation of BAT thermogenesis. In this study, a proteomics profile approach was used to figure out these hypothalamic intracellular signaling pathways in cold-exposed mice. As expected, numerous signaling pathways were triggered by cold stimulation, including the ErbB, GnRH, cAMP, Rap1, MAPK, insulin, PKG, Ras, and Ca^{2+} signaling pathways (Figure 2F,G), although we only verified the MAPK pathway role in the control of BAT thermogenesis. Further experiments are required for determination of the function of other hypothalamic signaling pathways in the regulation of BAT thermogenesis. In addition, IPA regulatory network analysis suggested that the MAPK pathway in the hypothalamus is likely associated with quantity of cells, movement disorders, and stabilization of microtubules. However, it is still unknown whether the MAPK pathway and its downstream DPPs indeed perform these roles in the POA. Further experiments are required to explore MAPK function in neural cells of the POA in the future.

Substantial studies have revealed that multiple hypothalamic signals such as AMP-activated protein kinase (AMPK), brain-derived neurotrophic factor (BDNF), cyclin-dependent kinase 4 (CDK4), and glucose-regulated protein (GRP78) regulate BAT thermogenesis [24–27]. Here, we discovered that p38α signaling in the POA is involved in thermoregulation. However, it is unclear whether p38α acting as a regulator of thermoregulation depends on BDNF, GRP78, CDK4, and AMPK signals or vice versa, and further experiments are required for the determination of how p38α signaling in the POA regulates BAT thermogenesis and of whether p38α also transduces BDNF, GRP78, CDK4, and AMPK signals to regulate BAT thermogenesis.

p38α is activated in response to a variety of extracellular stimuli and mediates signal transductions from the cell surface to the nucleus [14, 28]. Numerous studies have shown that p38α modulates metabolic processes in peripheral tissues such as insulin sensitivity, gluconeogenesis, adipogenesis, and lipolysis [15, 29]. p38α in BAT directly regulates BAT thermogenesis [30]. Upon cold exposure, catecholamines released by the sympathetic nervous system activate β3-adrenergic receptors (β3AR). β3AR stimulation is followed by activation of the cAMP/PKA signaling pathway, which is associated with increased expression of thermogenic genes in a p38α activation-dependent manner [8, 30]. Similarly, lacking p38α in adipose tissues lead to WAT browning, a lean phenotype, improved metabolism, and resistance to HFD-induced obesity [17]. Strikingly, in our study, p38α deletion in the POA ameliorated HFD-induced body weight gain, which was similar to that of mice lacking p38α in adipose tissue [17]. Despite a similar result in both models, the signaling pathway transduced by p38α in the POA is likely different from that in adipose tissue. In addition, there are many studies on the role of hypothalamic inflammation and endoplasmic reticulum stress in diet-induced obesity [31]. Overnutrition activates hypothalamic IκB kinase β (IKKβ)/nuclear factor-κB (NF-κB) signaling through elevating endoplasmic reticulum stress in the hypothalamus, whereas suppression of hypothalamic IKKβ/NF-κB signaling reduces the levels of HFD-induced weight gain [32]. Because p38α is also an inflammatory signal transducer and activates the IKKβ/NF-κB signaling pathway, it is unclear whether p38α in the POA for the maintenance of energy balance is also required for transmitting hypothalamic inflammation and endoplasmic reticulum stress signals.

Although the POA has always been characterized as a critical area in the control of body temperature homeostasis in response to ambient temperature change by modulating BAT thermogenesis [9, 10], the underlying signaling cascades are not fully understood. Our results showed that the phosphorylated p38α level in the POA was significantly decreased by cold exposure. Deletion of p38α in the POA increased the rectal and interscapular temperature of mice, as well as the expression of UCP1 and TH in BAT, and demonstrated an inhibitory effect of p38α in the POA for thermoregulation. However, it is unknown whether the inhibitory role of p38α for thermoregulation depends on its activity, and further experiments are required to investigate p38α activity in the POA.

Previous literature has shown that the POA is involved in the control of food intake in response to an ambient environment change [33, 34], whereas the roles of the POA in the control of energy

expenditure are fully unexplored. Studies have shed new light on the physiological function and the robust effect of the POA in energy expenditure [12]. Downregulated expression of G protein-coupled receptor 83 (GPR83) in warm-sensitive neurons of the POA reduces core body temperature and increases body weight gain of mice [35]. Some warm-sensitive neurons in the POA express leptin receptors and robustly modulate energy expenditure, body temperature, and food intake, which is involved in β3AR-dependent activation of BAT thermogenesis [11]. Consistently, in our study, the deletion of p38α in the POA increased mice body temperature and BAT thermogenesis, leading to a marked increase in energy expenditure and unchanged food intake. Therefore, the weight loss of mice with p38α deficiency in the POA is likely due to temperature-dependent metabolic adaptations but not food intake, and further experiments are required to elucidate the underlying physiological mechanism of p38α regulatory effect on temperature.

CONCLUSION

In summary, we found numerous hypothalamic signaling cascades in the regulation of BAT thermogenesis. Deletion of p38α in the POA protected against HFD-induced body weight gain and improved metabolic status, likely owing to an increase of BAT-mediated thermogenesis. Thus, all of these results demonstrate that p38α in the POA exacerbates obesity development at least in part via a decrease of BAT thermogenesis. These results also provide a potential target for the treatment of obesity in clinical practice.○

CONFLICT OF INTEREST
The authors declared no conflict of interest.

ORCID
Keke Lu https://orcid.org/0000-0002-2063-8250
Jiajun Zhao https://orcid.org/0000-0003-3267-9292
Zhao He https://orcid.org/0000-0003-0779-0052

REFERENCES
1. González-Muniesa P, Martínez-González MA, Hu FB, et al. Obesity. *Nat Rev Dis Primers*. 2017;3:17034. doi:10.1038/nrdp.2017.34.
2. Spiegelman BM, Flier JS. Obesity and the regulation of energy balance. *Cell*. 2001;104:531-543.
3. Tseng YH, Cypess AM, Kahn CR. Cellular bioenergetics as a target for obesity therapy. *Nat Rev Drug Discov*. 2010;9:465-482.
4. van Marken Lichtenbelt WD, Vanhommerig JW, Smulders NM, et al. Cold-activated brown adipose tissue in healthy men. *N Engl J Med*. 2009;360:1500-1508.
5. Peres Valgas da Silva C, Hernández-Saavedra D, White JD, Stanford KI. Cold and exercise: therapeutic tools to activate brown adipose tissue and combat obesity. *Biology (Basel)*. 2019;8:9. doi:10.3390/biology8010009
6. Bastías-Pérez M, Zagmutt S, Soler-Vázquez MC, Serra D, Mera P, Herrero L. Impact of adaptive thermogenesis in mice on the treatment of obesity. *Cells*. 2020;9:316. doi:10.3390/cells9020316
7. González-García I, Milbank E, Martinez-Ordoñez A, Diéguez C, López M, Contreras C. HYPOTHesizing about central comBAT against obesity. *J Physiol Biochem*. 2020;76:193-211.
8. Contreras C, Nogueiras R, Diéguez C, Medina-Gómez G, López M. Hypothalamus and thermogenesis: heating the BAT, browning the WAT. *Mol Cell Endocrinol*. 2016;438:107-115.
9. Morrison SF, Madden CJ, Tupone D. Central neural regulation of brown adipose tissue thermogenesis and energy expenditure. *Cell Metab*. 2014;19:741-756.
10. Morrison SF, Nakamura K. Central mechanisms for thermoregulation. *Annu Rev Physiol*. 2019;81:285-308.
11. Yu S, Qualls-Creekmore E, Rezai-Zadeh K, et al. Glutamatergic preoptic area neurons that express leptin receptors drive temperature-dependent body weight homeostasis. *J Neurosci*. 2016; 36:5034-5046.
12. Yu S, François M, Huesing C, Münzberg H. The hypothalamic preoptic area and body weight control. *Neuroendocrinology*. 2018;106: 187-194.
13. Hasegawa H, Meeusen R, Sarre S, Diltoer M, Piacentini MF, Michotte Y. Acute dopamine/norepinephrine reuptake inhibition increases brain and core temperature in rats. *J Appl Physiol (1985)*. 2005;99:1397-1401.
14. Han J, Wu J, Silke J. An overview of mammalian p38 mitogen-activated protein kinases, central regulators of cell stress and receptor signaling. *F1000Res*. 2020;9:F1000 Faculty Rev-653. doi:10.12688/f1000research.22092.1.
15. Nikolic I, Leiva M, Sabio G. The role of stress kinases in metabolic disease. *Nat Rev Endocrinol*. 2020;16:697-716.
16. He Z, Zhu HH, Bauler TJ, et al. Nonreceptor tyrosine phosphatase Shp2 promotes adipogenesis through inhibition of p38 MAP kinase. *Proc Natl Acad Sci U S A*. 2013;110:E79-E88.
17. Zhang S, Cao H, Li Y, et al. Metabolic benefits of inhibition of p38α in white adipose tissue in obesity. *PLoS Biol*. 2018;16:e2004225. doi:10.1371/journal.pbio.2004225.
18. Cao W, Daniel KW, Robidoux J, et al. p38 mitogen-activated protein kinase is the central regulator of cyclic AMP-dependent transcription of the brown fat uncoupling protein 1 gene. *Mol Cell Biol*. 2004;24: 3057-3067.
19. Hui L, Bakiri L, Mairhorfer A, et al. p38alpha suppresses normal and cancer cell proliferation by antagonizing the JNK-c-Jun pathway. *Nat Genet*. 2007;39:741-749.

20. Krämer AJ, Green J, Pollard J Jr, Tugendreich S. Causal analysis approaches in ingenuity pathway analysis. *Bioinformatics*. 2014;30: 523-530.

21. Tschöp MH, Speakman JR, Arch JR, et al. A guide to analysis of mouse energy metabolism. *Nat Methods*. 2011;9:57-63.

22. Huttlin EL, Jedrychowski MP, Elias JE, et al. A tissue-specific atlas of mouse protein phosphorylation and expression. *Cell*. 2010;143: 1174-1189.

23. Jing Y, Liu W, Cao H, Diéguez C. Hepatic p38α regulates gluconeogenesis by suppressing AMPK. *J Hepatol*. 2015;62:1319-1327.

24. López M, Nogueiras R, Tena-Sempere M, et al. Hypothalamic AMPK: a canonical regulator of whole-body energy balance. *Nat Rev Endocrinol*. 2016;12:421-432.

25. You H, Chu P, Guo W, Lu B. A subpopulation of Bdnf-e1-expressing glutamatergic neurons in the lateral hypothalamus critical for thermogenesis control. *Mol Metab*. 2020;31:109-123.

26. Castillo-Armengol J, Barquissau V, Geller S, et al. Hypothalamic CDK4 regulates thermogenesis by modulating sympathetic innervation of adipose tissues. *EMBO Rep*. 2020;21:e49807. doi:10.15252/embr.201949807.

27. Contreras C, González-García I, Seoane-Collazo P, et al. Reduction of hypothalamic endoplasmic reticulum stress activates browning of white fat and ameliorates obesity. *Diabetes*. 2017;66:87-99.

28. Hotamisligil GS, Davis RJ. Cell signaling and stress responses. *Cold Spring Harb Perspect Biol*. 2016;8:a006072. doi:10.1101/cshperspect.a006072.

29. Manieri E, Sabio G. Stress kinases in the modulation of metabolism and energy balance. *J Mol Endocrinol*. 2015;55:R11-R22.

30. Leiva M, Matesanz N, Pulgarín-Alfaro M, Nikolic I, Sabio G. Uncovering the role of p38 family members in adipose tissue physiology.

Front Endocrinol. 2020;11:572089. doi:10.3389/fendo.2020.572089.

31. Valdearcos M, Xu AW, Koliwad SK. Hypothalamic inflammation in the control of metabolic function. *Annu Rev Physiol*. 2015;77: 131-160.

32. Zhang X, Zhang G, Zhang H, Karin M, Bai H, Cai D. Hypothalamic IKKbeta/NF-kappaB and ER stress link overnutrition to energy imbalance and obesity. *Cell*. 2008;135:61-73.

33. Andersson B, Larsson B. Influence of local temperature changes in the preoptic area and rostral hypothalamus on the regulation of food and water intake. *Acta Physiol Scand*. 1961;52:75-89.

34. Brobeck JR. Food and temperature. *Recent Prog Horm Res*. 1960;16: 439-466.

35. Dubins JS, Sanchez-Alavez M, Zhukov V, et al. Downregulation of GPR83 in the hypothalamic preoptic area reduces core body temperature and elevates circulating levels of adiponectin. *Metabolism*. 2012;61:1486-1493.

SUPPORTING INFORMATION

Additional supporting information can be found online in the Supporting Information section at the end of this article.